Preoperative Planning Software for Corrective Osteotomy in Cubitus Varus and Valgus

João Tiago Pião Martins*

Thesis to obtain the Master of Science Degree in Biomedical Engineering

Supervisors: M.D. Cassiano Neves*[1] and Professor Joaquim Jorge*

*[1]Hospital CUF Descobertas

*Instituto Superior Técnico – Universidade de Lisboa (IST)

November 2016

Abstract: The supracondylar fracture of the humerus is the most common elbow lesion in children and it is the primary cause of cubitus varus and valgus. Although these deformations are mostly seen as a cosmetic issue, some studies showed that a continuous progression of these lesions can lead to more severe problems. Therefore an efficient corrective method is very important and the most used technique is a closing wedge osteotomy at the distal portion of the humerus.

The preoperative planning is usually made by using two radiographs, acquired at an anteroposterior and lateral views. The main problem with this 2D-approach relies on the fact that the deformation is three dimensional, which makes it very hard to fully correct the bone malformation with information from only two different angles.

In this thesis it was developed a software for the preoperative planning of a closing wedge osteotomy with medial displacement for cases of cubitus varus and valgus deformations. The novelty of the present work relies on the methodology used to plan this surgery, since it combined the usual radiographs with a 3D model of the distal portion of the humerus. This way, besides being possible to determine the corrective angles necessary for the planning of the osteotomy, this software can simulate as well this surgical approach and create a 3D representation of the postoperative humerus.

The feedback received from the tests performed with orthopaedics was very positive, showing that the presented software is a viable solution for the planning of the corrective surgery for this type of deformations.

Keywords: Cubitus Varus, Cubitus Valgus, Osteotomy, Geometric Modelling, Constructive Solid Geometry, Computer Aided Orthopaedic Surgery

I. INTRODUCTION

A. Problem Statement

In orthopaedics, a good preoperative planning can be the difference between a successful correction of a deformation or a not so successful surgery that will not re-established the functionality and the mobility of that anatomical structure. For that reason, in the last years many new approaches and techniques have emerged in this area, and one topic that is becoming more relevant is the use of computational techniques to perform the planning of the surgeries, which is referred as the Computer Aided Orthopaedic Surgery (CAOS) [1].

One of the simplest application for this type of technologies is the pre-operative planning using 3D bone surface modelling. This type of approaches can translate into a much more accurate and less invasive surgical interventions, and a better planning of the surgery [2]; it is also possible to simulate the preoperative plan that was defined to understand if it needs to be adjusted or not. This way, the use of these technologies can be determinant for the success of a surgery, especially orthopaedic corrective approaches, where there is a strong visual component associated to the preoperative planning. Finally, the CAOS systems can also give the doctor a previous knowledge of the anatomy of the bone and of the site where the surgery is being performed: with this knowledge, some complications and some unexpected surprises that could occur during the surgery can also be prevented.

The application developed in this work can be inserted into the universe of the CAOS technologies. What is presented here is an application developed to support the preoperative planning of the corrective osteotomy for cubitus varus and valgus deformations, and in which the user has access to a three dimensional model of the bone that can be used to simulate the surgery that was planned.

1) Cubitus Varus and Cubitus Valgus

Both varus and valgus deformities are characterized by an abnormal angle between two bones (according to the coronal plane) because of a wrong positioning of the distal portion of the bone in relation with the proximal portion of the other bone that the first is in touch with. The difference between these two is the value of the angulation that exists between the distal and the proximal parts: in the case of the varus deformity, the angle variation will lead to an approximation of distal bone to the middle line of the body; the valgus deformity will cause the opposite effect, with an increase of the distance to the middle line [3].

In the case of both cubitus varus and valgus, the most affected angle corresponds to the carrying angle of the elbow, which is the angle made, along the anteroposterior plane, between the humeral shaft and the forearm when the arm is fully extended and supinated [4]. There are many factors that can lead to the formation of these deformities, such as trauma, disease or congenital anomalies that affect the distal part of the humerus [5]. Among those, for the cubitus varus, the most common is the supracondylar fracture of the humerus [6]. In the case of the cubitus valgus, most of the cases result from a lateral condylar fracture of the humerus [5].

In most cases, these deformities do not affect the normal function of the elbow, being this way mostly a cosmetic problem [5]. However, these can lead to more severe problems. In the case of the cubitus valgus, the

continuous progression of the lesion can lead to the stretch of the ulnar nerve and therefore cause ulnar nerve palsy [7]. For the cubitus varus cases, the ulnar nerve palsy can also occur due to the continuous compression and subluxation of the nerve [5]. Other reports showed a relation between cubitus varus situation to posterolateral rotation instability, an internal rotation malalignment, pain and dislocation of the radial head [5,9].

Since the supracondylar fracture of the humerus is a common lesion in children, it only makes sense that this age group is the one with the higher prevalence of both cubitus varus and valgus. In fact, these type of deformities are very rare in adults [9,10].

2) Current Surgical Techniques

The treatment for both cubitus varus and valgus is through performing an osteotomy at the distal portion of the humerus. However, there are many variations of this surgical approach that can be used to correct these deformations, and all of them have different configurations for the osteotomy, different fixation methods and different approaches to the deformity [11].

The most common, simple and safer technique is the Lateral Closing Wedge Osteotomy with K-wire fixation. The biggest problem associated to this method is the increase of the prominence of the lateral condyle (in the case of cubitus varus) and of the prominence of the medial epicondyle (for the cubitus valgus).

An adaption of this approach that seems to reduce this prominence is the Lateral Closing Wedge Osteotomy with a medial displacement of the distal portion resulting from the osteotomy [5].

Another approach whose main goal is to deal with the prominence of the condyles is the Lateral Closing Wedge Osteotomy but with equal limbs [12], a method that, besides being able to resolve this issue, is not hard to reproduce. The Dome Osteotomy is another option [13], and is a different approach since the osteotomy is made along a semicircle, with an approximately 3cm radius, that is centred at a point situated 1cm distal from the olecranon.

The Step Cut Osteotomy [14] is also a viable option, since it makes it possible to avoid any type of lateral prominence. For adults, the Oblique Closing Wedge Osteotomy corresponds to a good alternative due to the increased area of contact between the proximal and distal parts after the osteotomy, which helps with the healing process of the bone [15].

Finally, there is also the Medial Opening Wedge Osteotomy with Bone Graft, where the correction of the deformity is based on the Illizarov technique. However, this technique has a high risk of damage to the ulnar nerve due to its lengthening and stretching [16].

The preoperative planning of the surgery in all these techniques is made based on radiographs acquired at an anteroposterior view (AP) and a lateral view. The AP radiograph is obtained with the elbow fully extended and the forearm supinated, while the lateral view one is obtained with a 90º elbow flexion and the palm and the forearm rested at a table [17]. To determine the corrective osteotomy angles, different measurements can be made: on the AP view, the carrying angle and the Baumann's angle can be measure; for the lateral view, the humerotrochlear angle is the one used.

The carrying angle of the elbow corresponds to the angle formed between the intersection of the long axis of the humeral shaft and the long axis of the forearm on the anteroposterior view [3].

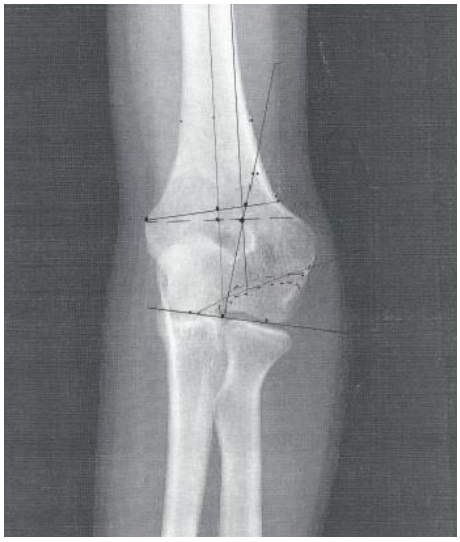

Figure 1 - Preoperative planning using and anteroposterior view radiograph to determine the deformity angles.

The Baumman's angle is obtained by the intersection of line that is perpendicular to the long axis of the humeral shaft with the line that is parallel to the lateral condyle.

Finally, the humerotrochlear angle is given by the intersection of the longitudinal line of the humeral shaft with the axis of the condyles.

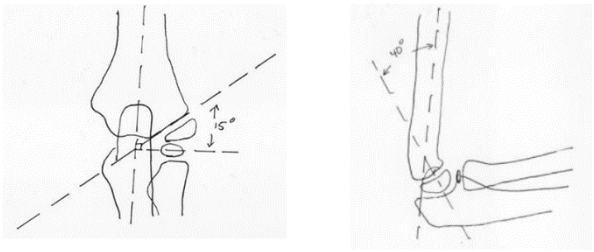

Figure 2 - Determining the Baumann's (left) and humerotrochlear (right) angles.

All of these angles can be determined by comparison to the correspondent angle measured on the healthy arm or to the standard values that are described at the literature: for children, is about 5º (to varus), 15º and 40º for the carrying angle, Baumann's angle and humerotrochlear angle, respectively.

The internal rotation of the deformity is also measured during the preoperative planning, and the most used method is the Yamamoto's one [18].

B. Literature Review

One of the biggest flaws of the current corrective approaches for both cubitus varus and valgus is the preoperative planning being done using only two radiographs when the deformities are three dimensional, which makes for any planning based on a 2D approach very hard to fully correct the bone malformations [19].

An area that seems to be in a great expansion around this subject is the planning of the corrective osteotomy using 3D imaging techniques that use sets of Computed Tomography (CT) images from both arms of the subjects

in order to plan the corrective surgery and simulate the aspect of the arm on the postoperative scene [19-26].

Although these 3D approaches provide a better assessment of the deformities, they have some disadvantages as well. One that is transversal to all these works is the increase of the radiation exposure of the patient, since it is necessary to perform, in most cases, two CT-scans, since the corrective angles and the osteotomy plan are obtained by superimposing the 3D models of both arms. Moreover, some of these works are only able to plan a simple lateral closing wedge osteotomy

C. Contribution of the Thesis

In an attempt to overcome these problems, in this work it was developed a software for preoperative planning of cubitus varus and valgus that is based on a novel technique that can be described as a mixture between the conventional planning that uses two radiographs and a three dimensional planning methodology that uses a 3D reconstruction of the deformed humerus. The planning of the corrective osteotomy is made by measuring both the Baumman's angle and the humerotrochlear angle on the two radiographs, like it is made when using the conventional planning: this way, with this approach it is not necessary a second CT-scan to the healthy arm to plan the corrective osteotomy. However, the value of these angles will be extrapolated to the 3D model, where it is possible to simulate the corrective osteotomy and see the final look of the bone. Furthermore, in this software it is also possible to estimate the necessary translation that is necessary to be applied to the distal portion in order to maintain the CORA.

II. GEOMETRIC MODELLING

In order to achieve a reliable simulation of the osteotomy is necessary to generate from the CT data set a 3D model that provides a very good approximation of the real bone. Thus, it was used the geometric modelling pipeline, described at Figure 3, to create this model, and which uses different software for each step [27,28].

A. Image Segmentation

Image segmentation can be defined as the clustering of the pixels of an image according to some criteria, like colour, intensity or texture, in order to partition the image into well-defined, homogeneous and with simple boundaries regions. The image segmentation is an essential aspect of any 3D reconstruction pipeline, since this process of regions separation is necessary to make it possible to reconstruct only the desired objects of an image [29].

There are many different image segmentation techniques that can be used according with the image that needs to be segmented: none of these techniques are good for every different type of images and not all of them are equally good for a certain type of image [30].

All of these techniques are also different in terms of automation: some of them are automatic, and others semi-automatic; it is also possible to perform manual segmentation, where the user manually selects the desired region. For the segmentation of CT images, there is not yet a fully automated method that can perform these images segmentation correctly [31].

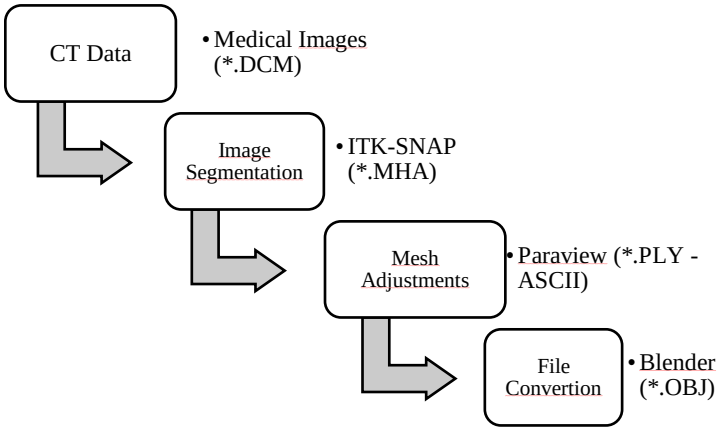

Figure 3 - Geometric modelling pipeline.

In the present work, the segmentation of the CT images was achieved by applying three different segmentation methods: global thresholding, active contour method and manual segmentation.

1) Global Thresholding

The global thresholding method performs the partition of the image based purely on the intensity values of each pixel. In this segmentation method, the user must choose the thresholds, minimum and maximum, for the intensity values, according with the histogram of the image: any pixel whose intensity lies between these two values will be consider as part of the region; otherwise, the pixel will be classified as background. This way, the global thresholding segments the image into a binary one.

This method has some negative aspects: for example, it is very sensitive to noisy images with artifacts, and does not take into account any spatial information of the image, thus preventing the extraction of only certain objects from the image.

2) Active Contour Model

The active contour model (or Snakes) corresponds to a segmentation method based on Partial Differential Equations (PDEs). In this method, the segmentation problem is converted into a PDE framework: the evolution of a certain curve, surface or image is translated into a PDE, and by solving that equations it will be possible to obtain the wanted solution for the problem [29,32].

The ITK-SNAP software [33] uses two different methods to perform the three dimensional active contour segmentation: the Geodesic Active Contours and Region Competition, and in both the segmented region is defined by contours (or snakes) [34]. Each contour corresponds to a closed surface $C(u, v, t)$, which is parameterized by the variables u, v and by the time t, and the movement of the curve is defined by the PDE showed at the equation below.

$$\frac{\partial}{\partial t} C(u, v, t) = F\vec{N} \qquad (1)$$

In this equation, the $\vec{N}$ corresponds to the normal vector of the contour and F defines all the forces that act upon the contour, which can either be internal or external forces: the internal forces are related with the geometry of the contour itself, and these are mainly used to impose restrictions in terms of the shape of the curve; on the other

hand, the external forces are associated with the characteristics of the image that is being segmented. For both geodesic active contours method and the region competition, the internal force that is taken in consideration is the mean curvature of the snake. However, these two methods use different parameters to define the external forces: in the case of the geodesic active contours method, it is taken in consideration the gradient magnitude of the intensity of the image [35]; for the region competition method, these external forces are based on voxel probability maps, and are therefore calculated by estimating, for each voxel of the image, the probability of it belonging to the structure of interest that is being segmented and the probability of that same voxel belonging to the background [27].

These active contour methods stop the segmentation when the snakes cannot evolve any further, due to the inexistence of more voxels to where they can expand, or when the user decide that the segmentation has already the desired appearance.

3) Manual Segmentation

With the two methods described previously it was possible to perform the majority of the segmentation process. However, there were still some regions that have yet to be correctly segmented, and in these cases it is necessary to resort to the manual segmentation.

In the ITK-SNAP software, the manual segmentation can be achieved by either drawing the desired area that the user wants segmented or by selecting individually the desired pixels.

B. Mesh Generation

In computer graphics, the representation of a model is achieved through the generation of a 3D Mesh. This mesh can be defined as a polyhedral volume formed by a set of nodes, edges and faces that usually correspond to simple polygons, such as triangles, quadrangles, tetrahedrons, among others. The mesh generation process corresponds to a bottom-up procedure: the nodes give origin to lines that form the surfaces, which will finally give origin to the mesh of the volume [27].

From the three dimensional image segmentation results a volume formed by binary voxels, in which each of those voxels will be a 0 or a 1, depending on whether belong to the structure or not. From this voxelized volume, the ITK-SNAP software is able to generate a 3D mesh using the marching cubes algorithm [36]. In this algorithm, each voxel will be seen as a 3D pixel that has an intensity value associated to, and the creation of the surface is done through a *divide-and-conquer* approach: a logical cube of eight pixels is created between two adjacent slices, and the intensity of each of those pixels will be compared to an isovalue; if in this cube there are voxels that have intensity values higher than the isovalue and others lower, then those voxels will contribute for the construction of the isosurface. This isosurface will be fully created by running this algorithm through all the cubes that can be defined between the adjacent slices. For each of those, if the cube has voxels that respect the previous conditions mentioned, then a surface, composed by triangular elements, will be created so that the voxels that are outside are separated from the ones that are inside [37].

The final isosurface will be formed by connecting all the surfaces that were defined, after passing through all the cubes. However, this mesh is not smooth; in fact, it has a very characteristic stair-step shape surface (Figure 4).

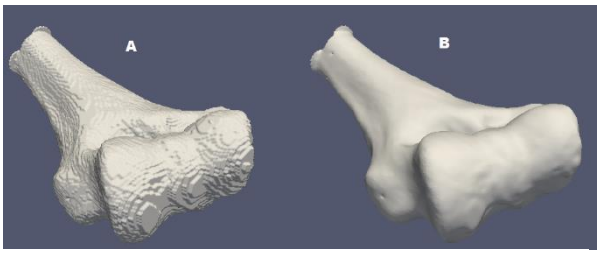

Figure 4 - Differences between the mesh of the distal humerus obtained from the marching cube algorithm (A) and after the Laplacian Smoothing (B).

1) Smoothing

To remove the rough appearance from the mesh it is necessary to perform its smoothing. This process is achieved by the application of a Low-Pass Filter, where the smoothing is performed in terms of the nodes positions in relation to their neighbour's position. This will lead to a change of the position of the nodes, and consequently of the shape of the triangle elements and of the surface, but without changing the number of nodes or faces.

In this work, the method used was the Laplacian smoothing, which is very efficient for rectifying the stair-step shape of a mesh [36]. The Laplacian smoothing corresponds to a neighbourhood processing method, where the allocation of the nodes is performed according to the position of the neighbour nodes.

2) Decimation

The surface mesh generated from the marching cube algorithm has a large amount of nodes and surfaces, many of which do not add any meaningful information to the geometry and topology of the mesh. In addition, this large number of points is inconvenient for the future computational methodology that is going to be done with this mesh. The Decimation Operation corresponds to a process of reducing the number of nodes and, consequently, of the triangles that form the surface mesh. Although this process does not keep the topology of the mesh, it provides a very good approximation of the original geometry.

The Decimation algorithm corresponds to an iterative method that will pass through all the nodes of the mesh multiple times. Each time that it passes through a node, this node will be treated as a possible candidate for removal: if it meets the decimation criteria that was established, then both the node and the triangular surfaces that were using that node are destroyed. This process leads to the creation of some holes in the mesh that are assessed though a local triangulation. At each iteration, this algorithm will continually delete nodes and triangles, adjusting at each passage the decimation criteria, until the percentage of decimation that was set by the user is achieved [38].

C. Constructive Solid Geometry (CSG)

The CSG corresponds to a modelling technique that allows the creation of a complex surface using Boolean operations [39]; for that reason, this method becomes very

useful when it is necessary to combine meshes or objects, which is exactly what was done on this work during the osteotomy simulation. In most CSG algorithms, the basic Boolean operations used are the union, intersection and difference (Figure 5).

In this work, the CSG implementation used was based on binary space partitioning trees (BSP trees), just like the implementation described at [39]. The BSP trees correspond to a very efficient spatial data structure which allows the application of Boolean operation into complex geometries in a fast way, due to the way the tree is structured. The binary space partition can be defined as a recursive operation that keeps continuously dividing a scene into two until a certain criterion is fulfilled; in this case, these trees were created from the recursive separation of a certain set of polygons according to their relative position to each other's, i.e. if the polygons are in front or at the back.

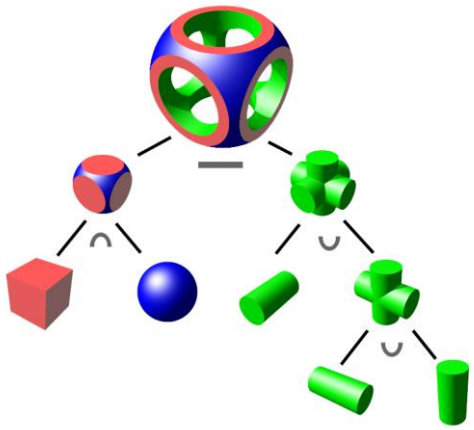

Figure 5 - Representation of the CSG tree algorithm, where the nods represent the Boolean operations: difference, intersection and union [40]

Simply put, the algorithm used to create the BSP tress can be divided into the following steps: first, a polygon from the list that contains all the polygons that define the mesh is chosen to be the root node of the tree; then, the rest of the polygons of the list will be divided among the two nodes that arise from this root node, where these will represent the group of polygons that are in front and the ones that are at the back of the root node; then, the same procedure is applied to the lists at the new formed nodes, and this procedure is repeated until there are no more lists to be split [39,41].

In order to apply the CSG Boolean operations with two (or more) geometries is necessary to create the correspondent BSP trees for each of them and merge those trees [39].

After the creation of the trees, it is necessary to create a list obtained by traversing one of the trees with the polygons that represent its boundaries. With this list, is now possible to find how the polygons of a model (for the sake of exemplification, A) will be classified on the BSP tree of the other model (B), which is also made through traversing the BSP tree of B; with this operation it will be obtained the list of polygons of model B that are inside and outside of A: by repeating this process to the other model, it is obtained the same list, but now with the polygons of A. From these two lists is now trivial to apply the desired Boolean operations.

III. Description of the Application

The application developed in this work, in the Unity platform [42], was designed for the preoperative planning of a closing wedge osteotomy with medial displacement of the distal portion of the humerus for both cubitus varus and valgus deformities.

The novelty of this application when comparing with similar ones described at literature relies on the fact that the planning of the corrective osteotomy is done by using both radiographs and a 3D model of the bone. This way, the application is formed by two distinct panels: a 2D panel, where all the planning related with the radiographs is done, and a 3D panel, where the 3D model of the distal portion of the humerus that was obtained from the CT data is presented and where the simulation of the osteotomy is performed.

A. 2D Panel

As shown in Figure 6, in the 2D Panel the user has access to the two radiographs that were taken to the arm of the patient with the deformity: one at an anteroposterior view (left) and another at a lateral view (right). This panel can

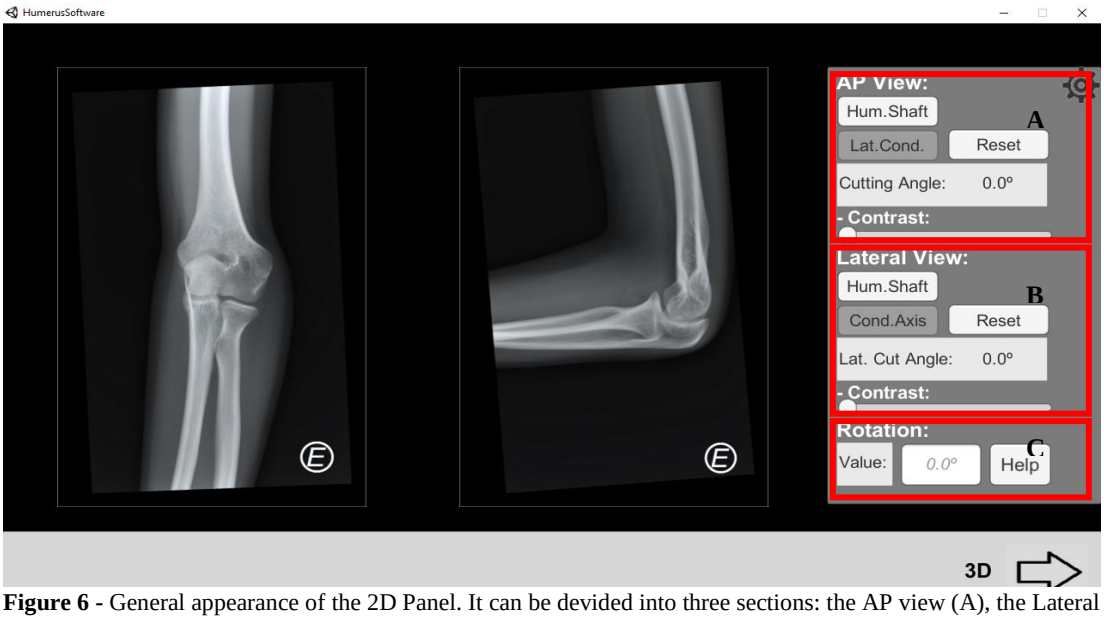

Figure 6 - General appearance of the 2D Panel. It can be devided into three sections: the AP view (A), the Lateral View (B) and the Rotation Commands (C).

be divided into three different sections, the AP View, the Lateral View and the Rotation: the first has all the functionalities and commands that are necessary to be used on the anteroposterior view radiograph, the second has the same but for the lateral view, and finally a section for determine the internal rotation of the deformation.

Similarly to what is done on the conventional methods, in this panel, from these two radiographs, the user will be able to determine both Baumann's angle and humerotrochlear angle, and from these two angles the corrective angles necessary to be applied will also be determined.

In order to determine the desired angles, the user has to draw on these radiographs certain lines. The method implemented for the creation of the lines is very simple: to each line, the user simply has to mark two points on the desired radiograph, i.e. the beginning and the end of the line. Although the methods for the determination of the Baumann's and humerotrochlear angles are different, the basic principle is the same: determining the angle made between two lines.

This way, in order to determine the angles from the lines drawn by the user, it was implemented a simple method: determine the vectors that define both lines, and then determine the angle made between those two vectors.

Another feature of this 2D Panel is the ability to manipulate both the radiographs that are presented, i.e. move them, zoom in and out and expand both of them into a larger window. All of these operations can be performed by the user by using fairly common commands, such as the mouse scroll wheel, double left click and right click of the mouse.

In this panel it is also possible to enhance the contrast of the radiographs, which can be applied by using the slider present at both AP and Lateral sections, which will affect the respective radiograph: this was achieved by manipulating the intensity gray values using a contrast stretching function.

Finally, since the data set that was used for testing this application did not have the radiographs of the healthy arm, in order to determine the corrective angles, the Baumann's and humerotrochlear angles that are determined are then compared to the normals values for these that are described in the literature (15º and 40º, respectively). However, under the settings button the user can change manually this reference values.

1) AP View Section

It is on the AP View Section that all the buttons and functionalities that are related with the anteroposterior radiograph are defined. As shown in Figure 1, the buttons that are defined in this section are all related with the creation of the necessary lines for the determination of the corrective angulation in the sagittal plane.

The angle that is determined on the AP radiograph to calculate the corrective angle necessary to be applied (according to the coronal plane) is the Baumannn's angle. Since the determination of the corrective angle from the Baumann's one is more suitable for children, it was decided to implement the calculation of the corrective angle based on this method, since the majority of the patients that suffer from these type of deformations are in fact children.

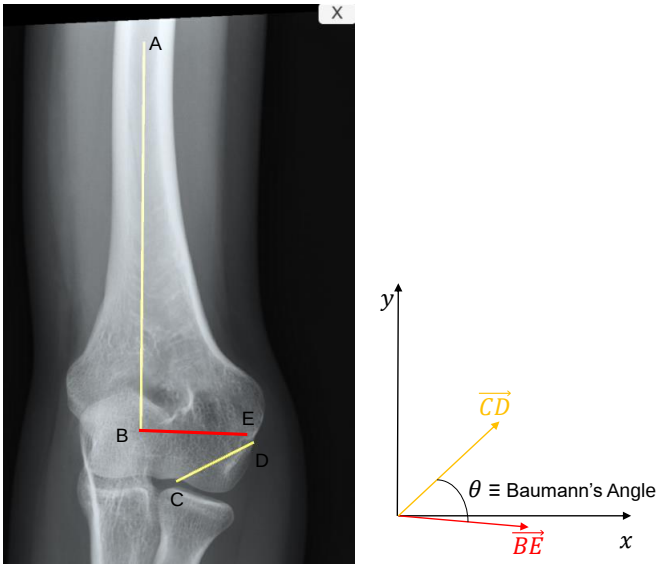

Figure 7 - Calculation of the Baumann's angle from the anteroposterior radiograph: the line segments $\overline{\boldsymbol{BA}}$ and $\overline{\boldsymbol{CD}}$ correspond to the humeral shaft axis and the lateral condyle axis drawn by the user, while the segment $\overline{\boldsymbol{BE}}$ represents the line perpendicular to $\overline{\boldsymbol{BA}}$; this way the Baumann's angle will correspond to the anlge made between the vectors $\overrightarrow{\boldsymbol{BE}}$ and $\overrightarrow{\boldsymbol{CD}}$.

All the buttons on the AP View Section are self-explanatory: the "Hum. Shaft" button can be used to draw the humeral shaft axis, the "Lat. Cond" to create a line parallel to the lateral condyle, and finally the "Reset" button to delete all previous marks that were made at this radiograph.

As already mentioned, the Baumann's angle corresponds to the angle made between the lateral condyle line and the line that is perpendicular to the humeral shaft axis. This way, after drawing the lines that are asked in the AP radiograph, the application will determine the perpendicular line to the line that represents the humeral shaft axis, and then it will determine the lowest angle possible between this new line and the lateral condyle segment that was also drawn, as shown in Figure 7. Finally, after determining the value of the Baumann's angle, the corrective angle will be determined by its comparison with the reference value that is defined on the application at that point.

2) Lateral View Section

The Lateral view section in terms of functionalities and commands is pretty similar to the AP view described previously, where the main difference is that on this section all these functionalities are used for the lateral view radiograph. As shown in Figure 6, in this section there are three different buttons that the user has access to: the "Hum. Shaft" button, which is used to mark the humeral shaft axis, the "Cond. Axis" button that is used to mark the axis of the condyles, and finally the "Reset" button that erases all the lines marked at this radiograph.

In this application the corrective angle necessary to be applied along the sagittal plane is obtained by measuring the humerotrochlear angle and comparing its value with the reference value that is defined for the humerotrochlear angle, i.e. the corrective angle will correspond to the difference between those two. As already described, the humerotrochlear angle corresponds to the angulation made between the humeral shaft axis and the condyle axis at the

lateral view radiograph. In Figure 8 is possible to see how this and the corrective angle are determined.

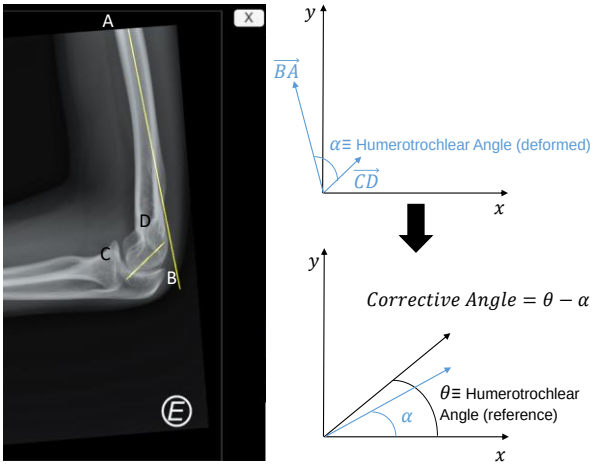

Figure 8 - Description of the method used for calculate the corrective angle based on the example presented: first, the humerotrochlear angle of the deformed arm is determined using the vector of the humeral shaft axis ($\overrightarrow{BA}$) and the condyle axis ($\overrightarrow{CD}$); then, this corrective angle is determined by comparing the angle calculated with the reference value set at the application.

3) Rotation Section

It is in this section that the user can determine the rotation value of the deformity. Usually, this value can be easily determined by the doctor on the patient using a goniometer, and for that reason it was implemented an option to manually insert this rotation value. However, it was also implemented another method to determine this rotation value, from a photo of the patient: this photo is taken at a lateral position, with the patient laid down with the arm abducted, the forearm flexed at 90º, and with the shoulder fully externally rotated. On this position, in normal subjects, the angle made between the forearm and the table where the subject is laid down is 0º; however, the same does not occur in subjects that have cubitus varus or cubitus valgus deformities. If this angle is superior to 0º, than it is necessary to apply an internal rotation of the distal part of the humerus; otherwise, if the angle made between the forearm and the table is negative, the correction that is necessary to be applied is an external rotation.

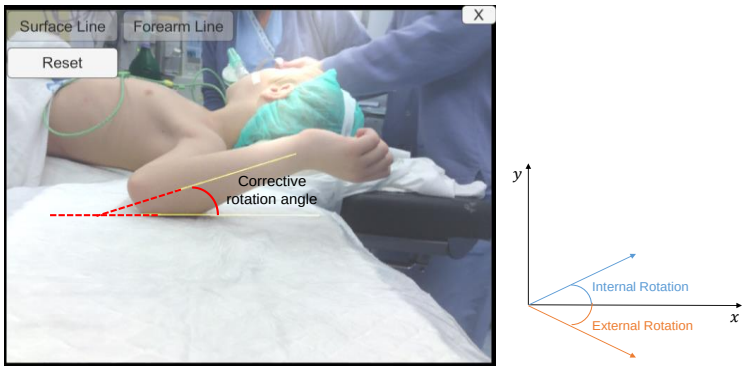

Figure 9 - Determination of the corrective rotation angle from the lines that were drawn: the surface line and the forearm line. The referential on the left represents when the angle measured will represent an internal rotation or an external rotation correction: the blue and orange vectors represent the forearm line, while the x axis represent the surface line.

After determining the corrective angles on both anteroposterior and lateral radiographs, as well as the internal rotative correction of the deformity, the user can advance to the 3D Panel of the application where the remaining steps of the planning of the osteotomy will be done.

B. 3D Panel

It is in the 3D Panel that the corrective osteotomy is planned and simulated in order to obtain the postoperative model of the bone; it is also where the translation that is necessary to be applied to the distal portion of the humerus in order to maintain the CORA of the elbow is calculated.

In order to fully plan the corrective osteotomy in the 3D Panel, the main steps that are necessary to be done are the creation of both cutting planes (distal and proximal), setting this way the osteotomy site, and determine the translation value for the medial displacement.

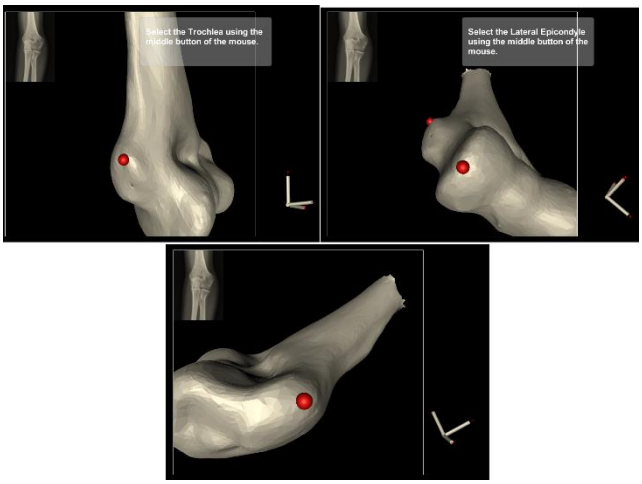

Figure 10 - Marking the three points on the model.

The first thing that has to be done in the 3D Panel is to mark the three points that are asked on the 3D model: a point at the medial epicondyle, another at the trochlea, and finally one at the lateral epicondyle, which will be used later to determine the translation necessary to be applied (Figure 10). After marking this points, the button "DC" becomes enabled and it is now possible to instantiate the distal cutting (DC) plane. The user can place this plane on the desired position for the osteotomy by applying translation and rotations along the the three axis, either using the window that pop-ups or the widget of the plane.

After creating the DC plane, the user can instantiate the proximal cutting (PC) plane with the button "PC". This plane when initiated will already be rotated according the corrective angles measured, and it will be anchored to the DC plane: this way, any translation applied to a plane will

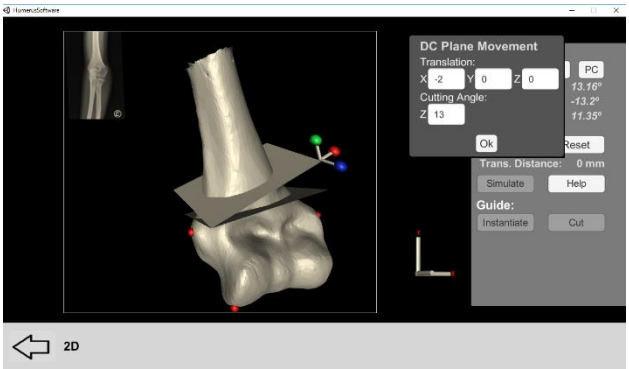

Figure 11 - Instantiating and positioning of the PC plane to the desired position. This plane will be anchored to the already created DC plane.

affect the other. In terms of rotation, there are fewer degrees of freedom.

After setting the osteotomy site by creating both DC and PC planes, it is now possible to determine the translation value that is necessary to be applied in order to maintain the CORA of the elbow joint. Similar to what was done in the 3D model, now the user has to mark the same points but on the AP radiograph. The reason for marking this two sets of points was to establish a spatial relation between the distal cutting plane instantiated in the 3D model and the correspondent vector on the radiograph.

In order to relate the 3D model with the 2D radiograph and to represent the DC plane through a 2D vector the main parameters that have to be found are the position and rotation of this plane relative to the bone. In order to find those parameters, the DC plane was treated as just a vector and it was represented by its middle line segment: this way it becomes easier to find a relation between the plane position and the points that were set on this 3D model.

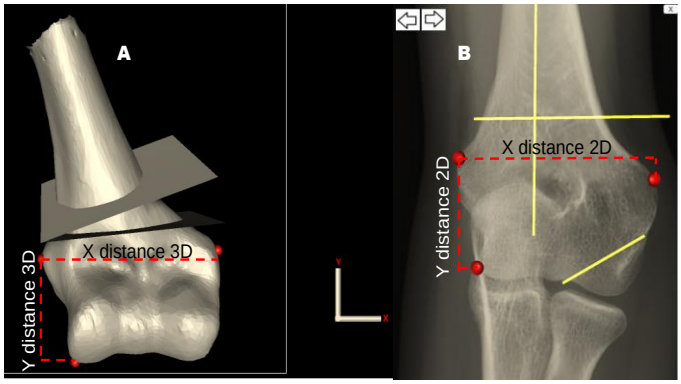

Figure 12 - Determination of the distance along x between the medial and lateral epicondyles and the distance along y between the medial epicondyle and the trochlea, in both 3D model (A) and 2D radiograph (B).

The position of this line relative to the bone was defined in terms of the distance along the x-axis between both the medial epicondyle and lateral epicondyle, and of the distance along the y-axis between the trochlear and medial epicondyle points (Figure 12). This way, by determining these distances in the 3D model and in the 2D radiograph it is possible to establish a conversion ratio between these two for both the x and y coordinates, according with equations 2 and 3.

$$Ratio_x = \frac{X\ distance\ 2D}{X\ distance\ 3D} \qquad (2)$$

$$Ratio_y = \frac{Y\ distance\ 2D}{Y\ distance\ 3D} \qquad (3)$$

From the ratios that were determined it is easy to find the point on the radiograph that corresponds to the medial point of the middle line of the DC plane (that corresponds to the point A at Figure 14): if the point A is defined as $A(X, Y, Z)$, then the correspondent point $a(x, y)$ on the AP radiograph will be given by:

$$a(x, y) = (X \times Ratio_x, Y \times Ratio_y) \qquad (4)$$

Now that is already known the position of the medial point of the DC plane on the AP radiograph is still necessary to discover the correspondent vector of this plane on the latter. Therefore, the method implemented for this purpose was to find a relation between the middle line of DC and the line segment that is defined by both medial and lateral epicondyle, i.e. find the angle that is made between the vector of the plane and the vector of the epicondyles line, on the 3D model.

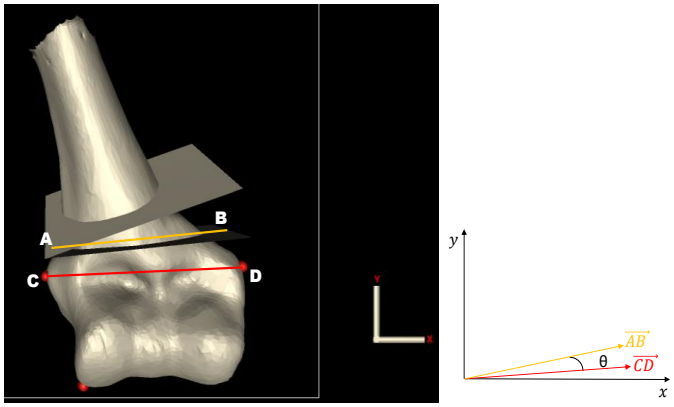

Figure 14 - Calculating the angle θ made between the line that connects both the epicondyles ($\overrightarrow{\mathbf{CD}}$) and the line that corresponds to the middle line of the plane DC ($\overrightarrow{\mathbf{AB}}$). For this calculus both vectors $\overrightarrow{\mathbf{AB}}$ and $\overrightarrow{\mathbf{CD}}$ are only defined in terms of x and y.

Once this angle is determined, it becomes easy to determine the vector correspondent to the DC plane on the radiograph: it is only necessary to find the vector that defines the line segment between the epicondyles in the AP view, and then rotate this vector by θ degrees around the z-axis. After determining this rotated vector on the radiograph, the creation of the desired line is simply obtained by applying this vector to the point that was obtained earlier.

After being created this line, the application determines the translation value, in millimetres, that is

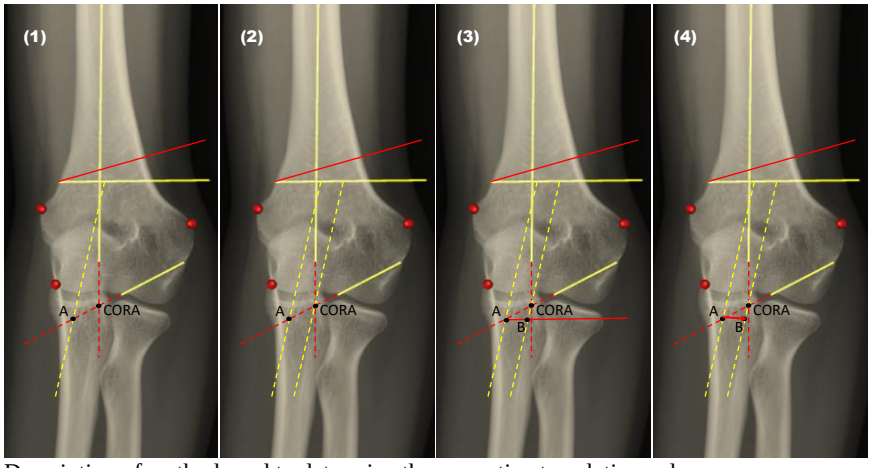

Figure 13 - Description of method used to determine the corrective translation value.

necessary to be applied. By using the arrows that are defined within the AP View window, the user has then the possibility to adjust the beginning of the line to the contour of the humerus in order to have a more accurate calculation of this translation value, since the osteotomy site should be set so that the end of the cutting wedge fits perfectly the contour of the humerus.

The translation value that is determined corresponds to the distance between the new CORA that is set if only the osteotomy is performed to the original CORA along the same direction of the vector that defines the DC line on the radiograph. The methodology implemented to determine this value from the lines is described in Figure 13.

After determining the corrective translation value, it is possible to simulate the osteotomy procedure and view the postoperative appearance of the bone. This simulation can be performed by clicking on the button "Simulate" present at the 3D Panel. The first step of this simulation correspond to the cutting of the bone according with the planes that were defined. To do so, it was necessary to create a three dimensional wedge mesh from these planes.

Depending on the value that was determined for the lateral cutting angle, the wedge model will have different appearances, as described at Figure 16. The method developed for the creation of this wedge model was pretty simple: each surface of the model was created individually, and then the full mesh was created by aggregating all of the surfaces that were defined. Each surface can be defined by only one polygon or by the combination of two, which can either be triangular or quadrangular polygons.

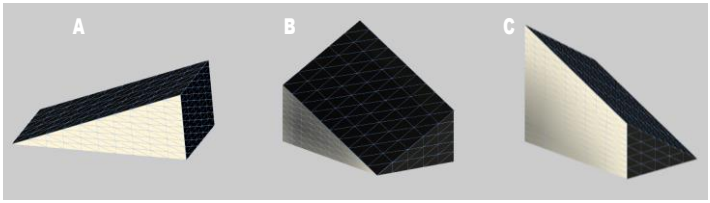

Figure 16 - Demonstration of the different wedge meshes that are generated according to the value of the lateral cutting angle: the wedge created when the angle is 0 (A), when the angle is positive (B) and when this angle is negative (C).

The process of cutting the 3D bone model with the wedge model that was created was achieved by using CSG Boolean Operations with those models; in this case, the operator that was applied was the difference between the bone and the wedge model. From the application of the difference operator, the bone will be split into two parts: a proximal part and a distal part. This way, in order to obtain the bone with the desired postoperative appearance it is still necessary to apply the rotations according to the cutting angles that were applied and the internal rotation of the deformity measured, as well as applying the translation and joining both distal and proximal parts. Therefore, the model that represents the bone on a postoperative scenario is only obtained after applying all these steps: each of these steps are applied individually and can be seen by the user on the simulation window that is open, as showed at FIG.

The remaining features of the 3D Panel are the possibility to create and position the screws that have to be inserted on the bone during the osteotomy for fixation purposes, as well as instantiate the guide, whose purpose was to be used during the surgery to facilitate the replication of the planning that was done with the application, and which should be set near the bone and in a way that it is intersected by both cutting planes and by both screws.

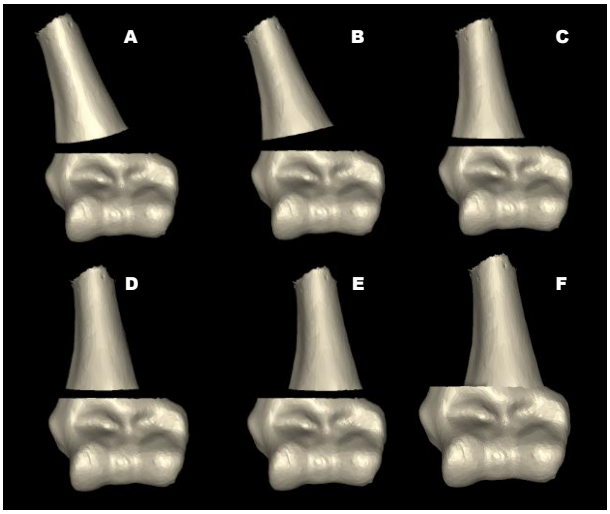

Figure 15 - Steps performed using the simulation of the osteotomy until the final postoperative look is achieved: (A) correspond the bone after performing the intersect Boolean operation, (B) is the bone after applying the lateral cut angle, (C) is after applying the cutting angle, (D) corresponds to the bone after rotating it according with the internal rotation of the deformity, (E) corresponds to the bone after the translation is applied, and finally (F) is the final appearance of the bone, with both distal and proximal parts joined together.

IV. RESULTS AND DISCUSSION

To evaluate the utility, viability and usability of the developed application it was necessary to perform some tests. Due to the nature and objective of the application, the participants that tested it were orthopaedists, as expected.

On total, one intern and two doctors specialized in orthopaedic tested the application, with the range of years of specialty varying from 8 to 36 years, and whose ages ranged between 25 and 65 years old. From these participants, all of them use regularly radiographs, and two thirds use these radiographs for the preoperative planning of corrective osteotomies. When questioned if they usually use three dimensional applications for the planning of this type of surgeries, most of them replied that they never use any software of this kind, with exception of one of the participants that replied that occasionally used.

The main tool used to evaluate the application was the Likert scale 6 questionnaire that the participants filled. Besides that, all participants were also submitted to a small interview, which provided a deeper insight of how the participants felt about the application.

By analysing the general feedback, the results obtained were very satisfactory: all of the participants found the application easy to use, useful for the planning of corrective osteotomies and more precise than the conventional methods.

On the 2D Panel, all the participants thought that the methodologies used to determine the corrective angles from the radiographs were appropriate and easy to perform. Only the method used to determine the internal rotation of the deformity was not well received by all the participants, since one thought that the method used was not the most adequate.

For the 3D Panel, all the participants seemed to be comfortable with the commands used for the rotation and translation of the 3D model, and also with the methods

used to position both distal and proximal cutting planes along the bone model. Once again, there was only one functionality of this panel in which the responses were not uniform, and it was the question related with the methodology used to determine the translation value: even though all the participants found it to be very useful, not all were fully certain if the methodology was the most appropriate. Finally, all of them appreciated the simulation of the osteotomy and to be able to visualize the postoperative appearance of the humerus.

From the responses given to the interviews, it was possible to obtain some interesting opinions relative to the conventional methods and the application being tested. Most of the participants said that the conventional methods are not the most accurate or precise methods, but that it is possible to achieve good results when the orthopaedist is already very experienced. Similarly to what was seen from the answers given to the questionnaire, all the participants thought that the application was easy to use and that it could be more advantageous for the planning of the corrective osteotomy when compared to the conventional methods, especially for doctors that are less experienced. Also it is found to be faster than the conventional methods and that the three dimensional visualization of the bone is interesting and can be very useful. Finally, all the participants thought that the presented solution was a viable option for the preoperative planning of other type of deformations as well.

However, it is also important to mention the fact that the results presented may not truly reflect the real and correct evaluation of this application due to the sample size being too small. Nonetheless, the responses and the feedback obtained during the tests were very motivating and satisfactory, demonstrating that the application presented in this work is a viable solution for the planning of the corrective osteotomy in cases of cubitus varus and valgus deformations, and can even be more accurate, easier and faster than the conventional methods that are being used nowadays, fulfilling perfectly its purpose.

V. CONCLUSIONS AND FUTURE WORK

The main goal of this work was to develop an application for the preoperative planning of corrective surgery in cases of cubitus varus and valgus deformations that would be based on a three dimensional model of the bone with the deformity, and through this model simulate the osteotomy, which would provide an approximation model of the postoperative look of the distal portion of the humerus. The novelty of the present work when compared to similar ones in this area relies on the method used to determine the corrective angles for the osteotomy: instead of determining the corrective angles by superimposing the 3D models of the deformed with the healthy arm, the methodology proposed in this work combines the two radiographs that are acquired for the conventional methods with the 3D model of the deformed armed.

With the final version developed it was possible to fully plan the corrective osteotomy for a given case of cubitus varus: from the two radiographs presented at the 2D Panel, both cutting angles were determined with accuracy, and the methodology used to determine the internal rotation of the deformity was adequate and functional; on the 3D Panel, the 3D model of the bone

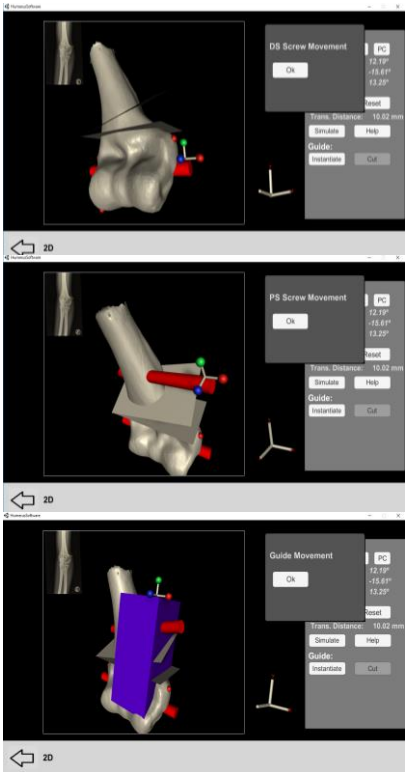

Figure 17 - Representation on the 3D scene of both distal screw (DS) and proximal screw (PS), as well as the guide.

allowed to set the osteotomy site more easily and to perform a simulation of the corrective osteotomy, in order to obtain the model of the distal humerus on a postoperative scenario; in addition, the application allowed to determine the translation value that is necessary to be applied during the surgery to the distal portion of the humerus in order to maintain the CORA of the elbow joint.

From the tests performed, although the number of participants that integrated the study was low, the majority believed that this application could lead to a more accurate, faster and easier planning of the surgery when compared to the conventional methods that are used nowadays, especially for less experienced orthopaedics.

Despite all the positive feedback that was received, the application still had its flaws, since it was possible to find some bugs and functionalities that were not working as intended during the tests.

Therefore, in order to continue improving the application presented in this work, fixing these flaws should be the number one priority on future work list. Besides that, the sample size used for the testing of the application should be increased, in order to fully validate the methodology used for this planning and also to receive more and different feedbacks and suggestion from specialists in this area. Another feature that should be added to the application in the future is the creation of the customized guide, i.e. a guide that would be specifically made for the patient and which would have the holes for the insertion of the fixation screws and the spaces for the saws used to perform the cuts on the humerus, essential to ensure that the surgery was performed exactly as planned on the application. Finally, after validating this application, something that should definitely be taken into consideration is the development of similar applications and methodologies for other types of deformities on other bones of the body.

VI. References

[1] Joskowicz, Leo, and Eric J. Hazan. "Computer Aided Orthopaedic Surgery: Incremental shift or paradigm change?" *Medical Image Analysis* 33 (2016): 84-90.

[2] Schep, N.W.L., I.A.M.J. Broeders, and Chr. van der Werken. "Computer assisted orthopaedic and trauma surgery." *Injury* 34 (2003): 299-306.

[3] Oestreich, Alan E. *How to Measure Angles from Foot Radiographs.* New York: Springer-Verlag, 1990.

[4] Benson, Michael, John Fixsen, Malcom Macnicol, and Klaus Parsch. *Children's Orthopaedics and Fractures.* Third. London: Springer, 2010.

[5] Joseph, Benjamin, Selva Nayagam, Randall Loder, and Ian Torode. *Pediatric Orthopaedics: A System of Decision-Making.* Second Edition. Boca Raton: CRC Press, 2016.

[6] Morrissy, Raymond T., and Stuart L. Weinstein. *Atlas of Pediatric Orthopaedic Surgery.* Fourth Edition. Philadelphia: Lippincott Williams & Wilkins, 2006.

[7] Guardia, Charles F. "Ulnar Neuropathy: Background, Anatomy, Pathophysiology." *Medscape.* 20 Jul 2016. http://emedicine.medscape.com/article/1141515-overview (accessed Sep 6, 2016).

[8] Srivastava, Amit, Anil Kumar Jain, Ish Kumar Dhammi, and Rehan Ul Haq. "Posttraumatic progressive cubitus varus deformity managed by lateral column shortening: A novel surgical technique." *Chinese Journal of Traumatology* 19 (2016): 229-230.

[9] Piggot, James, H. Kerr Graham, and Gerald F. McCoy. "Supracondylar Fractures of the Humerus in Children." *British Editorial Society of Bone and Joint Surgery* 68 B (1986): No. 4.

[10] Bonczar, Mariusz, Daniel Rikli, and David Ring. *AO Surgery Reference.* n.d. https://www2.aofoundation.org (accessed Sep 6, 2016).

[11] Tanwar, Yashwant S., Masood Habib, Atin Jaiswal, Satyaprakash Singh, Rajender K. Arya, and Skand Sinha. "Triple modified French osteotomy: a possible answer to cubitus varus deformmity. A technical note." *Journal of Shoulder and Elbow Surgery* 23 (2014): 1612-1617.

[12] El-Adl, Wael. "The equal limbs lateral closing wedge osteotomy for correction of cubitus varus in children." *Acta Orthopaedica Belgica* 73 (2007): 5.

[13] Hahn, Soo Bong, Yun Rak Choi, and Ho Jung Kang. "Corrective dome osteotomy for cubitus varus and valgus in adults." *Journal of Shoulder and Elbow Surgery* 18 (2009): 38-43.

[14] Bali, K., P. Sudesh, A. Sharma, S.R.R. Manoharan, and A.K. Mootha. "Modified step-cut osteotomy for post-traumatic cubitus varus: Our experience with 14 children." *Elsevier Masson*, May 2011.

[15] Gong, Hyun Sik, Moon Sang Chung, Joo Han Oh, Hoyune Esther Cho, and Goo Hyun Baek. "Oblique Closing Wedge Osteotomy and Lateral Plating for Cubitus Varus in Adults." *Clinical orthopaedics and related research* 466.4 (2008): 899-906.

[16] Babhulkar, Sudhir. *Elbow Injuries.* New Delhi: Jaypee Brothers Medical Publishers, 2015.

[17] Park, Shinsuk, and Eugene Kim. "Estimation of carrying angle based on CT images in preoperative surgical planning for cubitus deformities." *Acta Medica Okayama* 63.6 (2009): 359-365.

[18] Yamamoto, Isao, Seiichi Ishii, Masamichi Usui, and Toshihiko Ogino. "Cubitus Varus Deformity Following Supracondylar Fracture of the Humerus: A Method for Measuring Rotational Deformity." *Clinical orthopaedics and related research* 201 (1985): 179-185.

[19] Omori, Shinsuke, et al. "Three-dimensional corrective osteotomy using a patient-specific osteotomy guide and bone plate based on a computer simulation system: accuracy analysis in a cadaver study." *The International Journal of Medical Robotics and Computer Assisted Surgery* 10.2 (2014): 196-202.

[20] Oka, Kunihiro, et al. "Accuracy of corrective osteotomy using a custom-designed device based on a novel computer simulation system." *Journal of Orthopaedic Science* 16.1 (2011): 85-92.

[21] Zhang, Yuan Z., Sheng Lu, Bin Chen, Jian M. Zhao, Rui Liu, and Guo X. Pei. "Application of computer-aided design osteotomy template for treatment of cubitus varus deformity in teenagers: a pilot study." *Journal of Shoulder and Elbow Surgery* 20.1 (2011): 51-56.

[22] Bryunooghe, Els. "Case studies using 3D technologies for corrective osteotomies: synergy between engineer and surgeon." *BMC Proceedings* Vol. 9. No. 3. BioMed Central (2015).

[23] Takeyasu, Yukari, et al. "Three-dimensional analysis of cubitus varus deformity after supracondylar fractures of the humerus." *Journal of Shoulder and Elbow Surgery* 20(3) (2011): 440-448.

[24] Oka, Kunihiro, Tsuyoshi Murase, Hisao Moritomo, and Hideki Yoshikawa. "Corrective osteotomy for malunited both bones fractures of the forearm with radial head dislocations using a custom-made surgical guide: two case reports." *Journal of Shoulder and Elbow Surgery* 21.10 (2012): e1-e8.

[25] Omori, Shinsuke, et al. "Postoperative accuracy analysis of three-dimensional corrective osteotomy for cubitus varus deformity with a custom-made surgical guide based on computer simulation." *Journal of Shoulder and Elbow Surgery* 24.2 (2015): 242-249.

[26] Tricot, Mathias, Khanh Tran Duy, and Pierre-Louis Docquier. "3D-corrective osteotomy using surgical guides for posttraumatic distal humeral deformity." *Acta Orthopaedica Belgica (Bilingual Edition)* 78.4 (2012): 538-542.

[27] Lopes, Daniel Simões. "Geometric Modeling of Human Structures Based on CT Data–a Software Pipeline." 2006.

[28] Lopes, Daniel Simões. "Smooth convex surfaces for modeling and simulating multibody systems with compliant contact elements." 2013.

[29] Dass, Rajeshwar, Priyanka, and Swapna Devi. "Image Segmentation Techniques." *IJECT* 3.1 (Jan - March 2012).

[30] Pal, Nikhil R., and Sankar K. Pal. "A review on image segmentation techniques." *Pattern recognition* 26.9 (1993): 1277-1294.

[31] Sharma, Neeraj, e Lalit M. Aggarwal. "Automated medical image segmentation techniques." *Journal of medical physics* 35.1 (2010): 3.

[32] Jiang, Xin, Renjie Zhang, and Shengdong Nie. “Image segmentation based on PDEs model: A survey.” *3rd International Conference on Bioinformatics and Biomedical Engineering.*, 2009.

[33] *ITK-SNAP*. 2016. http://www.itksnap.org/pmwiki/pmwiki.php (accessed May 26, 2016).

[34] Yushkevich, Paul A., et al. “User-guided 3D active contour segmentation of anatomical structures: significantly improved efficiency and reliability.” *NeuroImage* 31 (2006): 1116-1128.

[35] Caselles, Vicent, Ron Kimmel, and Guillermo Sapiro. “Geodesic Active Contours.” *International Journal of Computer Vision* 22(1) (1997): 61-79.

[36] Ribeiro, N. S., P. C. Fernandes, D. S. Lopes, J. O. Folgado, e P. R. Fernandes. “3-d solid and finite element modeling of biomechanical structures-a software pipeline.” *Proceedings of the 7th EUROMECH Solid Mechanics Conference*, 2009.

[37] Lorensen, William E., and Harvey E. Cline. “Marching cubes: A high resolution 3D surface construction algorithm.” *ACM siggraph computer graphics.* 21 (1987).

[38] Schroeder, William J., Jonathan A. Zarge, and William E. Lorensen. “Decimation of triangle meshes.” *ACM Siggraph Computer Graphics.* 26 (1992).

[39] Segura, Christian, Taylor Stine, e Jackie Yang. “Constructive Solid Geometry Using BSP Tree.” 2013.

[40] *Wikipedia, the free encyclopedia: Constructive Solid Geometry.* 2016. https://en.wikipedia.org/wiki/Constructive_solid_geometry (accessed 14 Oct, 2016).

[41] Funchs, Henry, M. Kedem Zvi, and F. Naylor Bruce. “On visible surface generation by a priori tree structures.” *ACM Siggraph Computer Graphics.* 14 (1980).

[42] *Unity*. n.d. https://unity3d.com/pt (accessed March 23, 2016).